ChemPubSoc Europe

DOI: 10.1002/chem.201303885

CHEMISTRY
A European Journal
Full Paper

Host–Guest Systems

Origins of Large Rate Enhancements in the Nazarov Cyclization Catalyzed by Supramolecular Encapsulation

Courtney J. Hastings,[a, b] Robert G. Bergman,*[a, b] and Kenneth N. Raymond*[a, b]

Abstract: The self-assembled supramolecular host $[Ga_4L_6]^{12-}$ (**1**; L = *N,N*-bis(2,3-dihydroxybenzoyl)-1,5-diaminonaphthalene) catalyzes the Nazarov cyclization of 1,3-pentadienols with extremely high levels of efficiency. The catalyzed reaction proceeds at a rate over a million times faster than that of the background reaction, an increase comparable to those observed in some enzymatic systems. A detailed study was conducted to elucidate the reaction mechanism of both the catalyzed and uncatalyzed Nazarov cyclization of pentadienols. Kinetic analysis and ^{18}O-exchange experiments implicate a mechanism, in which encapsulation, protonation, and water loss from substrate are reversible, followed by irreversible electrocyclization. Although electrocyclization is rate determining in the uncatalyzed reaction, the barrier for water loss and for electrocyclization are nearly equal in the assembly-catalyzed reaction. Analysis of the energetics of the catalyzed and uncatalyzed reaction revealed that transition-state stabilization contributes significantly to the dramatically enhanced rate of the catalyzed reaction.

Introduction

There are strong parallels between host–guest dynamics and ligand–receptor interactions of biomacromolecules, and considerable effort has been made to develop synthetic analogs of important biochemical processes.[1] This analogy is even more apt for self-assembled hosts; the three-dimensional structure of a protein is dictated by its primary amino acid sequence, while the structure of a self-assembled molecule is programmed by the geometrical relationships and functional groups present in each subunit. Enzymes, in particular, have captivated chemists with their ability to catalyze reactions with extremely high levels of selectivity and activity under mild, aqueous conditions, and much effort has gone into developing supramolecular catalysts that mimic enzymatic function.[2] Such catalysts rely upon noncovalent interactions to provide the primary associative interaction between catalyst and substrate, one factor that is responsible for the spectacular selectivity and reactivity of enzymes.

The self-assembled metal–ligand assembly $[Ga_4L_6]^{12-}$ (**1**; L = *N,N*-bis(2,3-dihydroxybenzoyl)-1,5-diaminonaphthalene; Figure 1) can act as a host for suitably sized cationic and neutral guest molecules.[3] The host ligand framework generates a large, hydrophobic interior cavity (250–450 Å^3) that can encapsulate guest molecules with binding affinities of up to 10^5 M^{-1}.[4] The properties of **1** have been exploited to develop reactions that occur inside the cavity of **1** with higher degrees of reactivity than when the reaction is performed in bulk solution. For example, inclusion of reactive allyl enammonium cations in **1** greatly increases the rate of the 3-aza Cope rearrangement by binding a folded conformation of the reactant that resembles the transition state of the reaction.[5] Encapsulation in polyanionic **1** can perturb certain chemical equilibria to favor the formation of cationic species, such as iminium ions and labile phosphonium adducts.[6] This equilibrium shift also applies to a wide range of protonated amines and phosphines that are encapsulated in **1**, even at strongly basic pH. The effective basicity of guest molecules is enhanced between 2.1 and 4.5 orders of magnitude. These investigations led to the

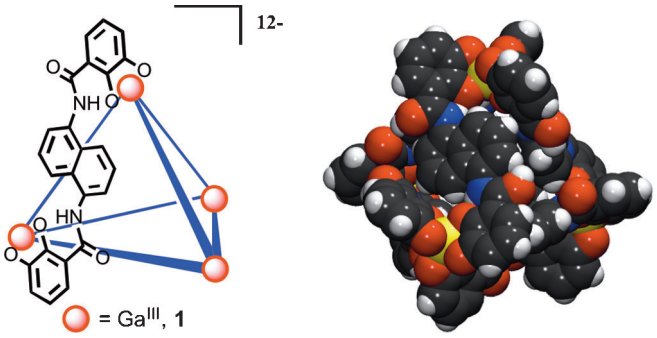

Figure 1. Left: schematic view of **1**, in which the bis-bidentate ligands are represented by blue lines and the gallium atoms are represented by red circles. Right: space-filling model of **1**.

[a] Dr. C. J. Hastings, Prof. R. G. Bergman, Prof. K. N. Raymond
Department of Chemistry, University of California
Berkeley, CA 94720-1416 (USA)
Fax: (+1) 510-642-7714
Fax: (+1) 510-486-5283

[b] Dr. C. J. Hastings, Prof. R. G. Bergman, Prof. K. N. Raymond
Lawrence Berkeley National Laboratory
1 Cyclotron Road, Berkeley, CA 94720 (USA)
E-mail: rbergman@berkeley.edu
raymond@socrates.berkeley.edu

Supporting information for this article is available on the WWW under http://dx.doi.org/10.1002/chem.201303885.

development of proton-catalyzed hydrolysis reactions inside **1**, in which a protonated transition state is stabilized in the host interior.[7] These reactions are remarkable in that there are no functional groups in the interior of **1**; the protonation of bound guests, as well as the transition states for their subsequent reactions, are favorable due to the charge of the host assembly and cation–pi interactions with the naphthalene rings of the host walls.[8] The stabilization of transient protonated species produces a several thousand-fold rate acceleration of orthoformate and acetal hydrolysis under basic conditions.

We have communicated early studies of the Nazarov cyclization of 1,4-pentadien-3-ols (e.g., compound **2** in Scheme 1a–),

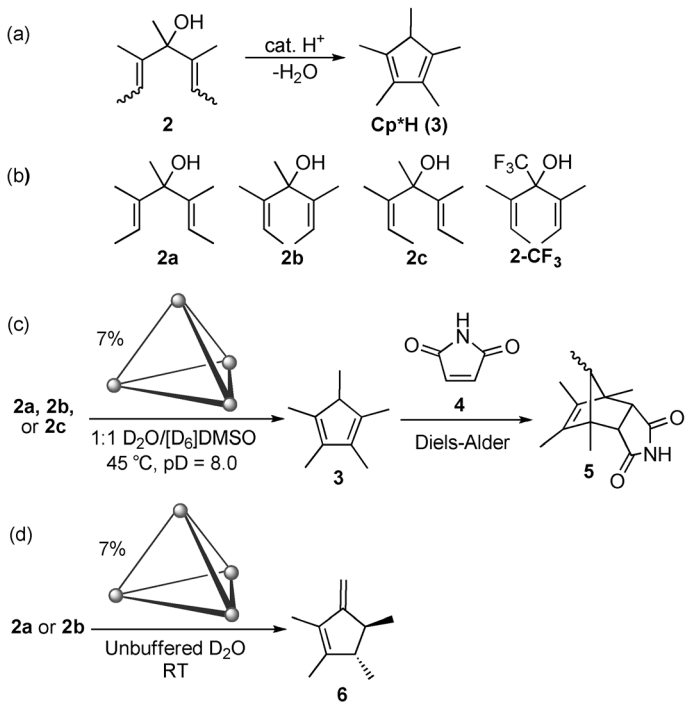

Scheme 1. a) General Scheme for the Nazarov cyclization of pentadienols to form cyclopentadienes. b) Pentadienol stereoisomers used in this study. c) **1**-Catalyzed Nazarov cyclization with maleimide (**4**) added to convert Cp*H (**3**) to weakly binding Diels–Alder adduct **5**, alleviating product inhibition. d) Formation of unexpected dihydrofulvene isomer **6** from the **1**-catalyzed reaction of symmetrical substrates **2a** or **2b**.

a reaction that is catalyzed by supramolecular encapsulation within **1**.[9] The rate of the catalyzed reaction is up to 2100000 times larger than that of the uncatalyzed reaction, representing one of the largest reported rate accelerations for a reaction catalyzed by supramolecular encapsulation (Table 1). This is a rare example of supramolecular catalysis that achieves a level of rate enhancement comparable to that observed in several enzymes.[10] The reaction proceeds in aqueous or mixed water/DMSO solution at near-neutral pH and mild temperature. The reaction product, pentamethylcyclopentadiene (Cp*H, **3**), is a suitable guest for **1**, and causes product inhibition when the catalyzed reaction is carried out in mixed water/DMSO solution. Addition of maleimide to the reaction mixture traps Cp*H as the corresponding Diels–Alder adduct **5**, the binding constant of which is low enough that it does not bind competitively with substrate (Scheme 1c). The unexpected formation of dihydrofulvene **6** in the **1**-catalyzed Nazarov cyclization of symmetrical substrates **2a** and **2b** was recently disclosed (Scheme 1d). The formation of **6** instead of its expected regioisomer **3** is the result of a kinetically controlled, regioselective deprotonation of an intermediate cyclopentenyl carbocation.[11] The regioselectivity of this deprotonation step is determined by encapsulation within **1**; no regioselectivity was observed when the reaction was conducted in free solution. Herein, we present mechanistic studies of the host-catalyzed Nazarov cyclization that were conducted to elucidate the reaction mechanism of both the catalyzed and the uncatalyzed reaction. Quantifying the energy profile of both reactions provides insight into the dramatic and unprecedented rate acceleration of the **1**-catalyzed reaction over the uncatalyzed reaction.

Table 1. Kinetic data for Nazarov substrates.[a]

Substrate	k_{cat} [s^{-1}]	k_{uncat} [s^{-1}]	Rate acceleration (k_{cat}/k_{uncat})
2a[b]	$(2.9(4)\times10^{-2})$	$4.0(3)\times10^{-8}$	(730000)
2b	$1.6(1)\times10^{-2}$	$7.7(8)\times10^{-9}$	2100000
2c	$5.7(1)\times10^{-2}$	$3.3(1)\times10^{-8}$	1700000

[a] Reactions conducted at 45 °C in D_2O/[D_6]DMSO 1:1. Standard errors are given in parentheses. [b] The k_{cat} and rate acceleration values for substrate **2a** (in parentheses) were estimated from competitive binding experiments with **2c** (see the Supporting Information for a detailed discussion).

Results and Discussion

Kinetic studies of the 1-catalyzed reaction

To probe the origin of the rate enhancement of the **1**-catalyzed Nazarov cyclization, mechanistic analysis of both the **1**-catalyzed and the uncatalyzed reaction were conducted, focusing on whether the transition state of the rate-determining step is stabilized by the constrictive interior of **1**. Mechanistic studies were conducted by using **2b** as a substrate. Pseudo-first-order consumption of starting material was observed under **1**-catalyzed conditions.[9] Variable-concentration kinetic studies of the catalytic reaction revealed a first-order dependence on [**1**] (Figure 2) and an apparent order of 0.5 on [D^+] (Figure 3, see below). The catalyst resting state was determined to be the encapsulated, neutral substrate **2b**⊂**1** (in which ⊂ denotes encapsulation) by ^{13}C NMR analysis, and the self-exchange rate[12] k_{exch} of **2b** in **1** is 2.4 s^{-1}, which is fast relative to the overall rate of the **1**-catalyzed reaction.[9] Kinetic studies of the uncatalyzed reaction of substrate **2b** were also conducted; these display first-order dependence on both substrate concentration and [D^+] (Figure 4).[13] Additional data are provided by the reactivity of the substrate **2-CF$_3$** (Scheme 1b), which is similar in size to **2b**, but much less basic than **2b** owing to the electron-withdrawing trifluoromethyl substituent.[14] No reaction occurred when the **1**-catalyzed Nazarov cyclization of **2-CF$_3$** was attempted, although the expected host–guest complex **2-CF$_3$**⊂**1** was immediately formed. Taken together, these data implicate a mechanism that involves rapid,

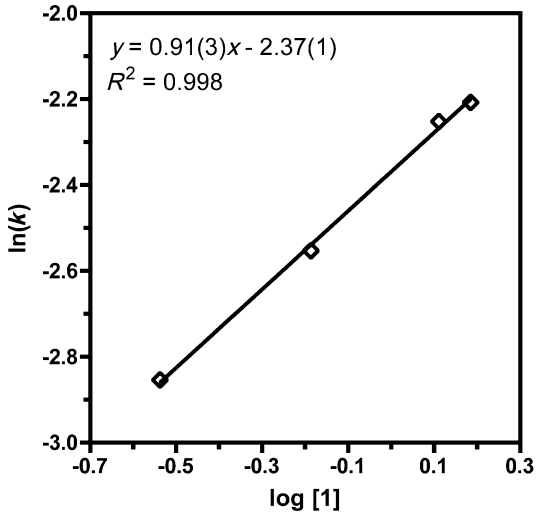

Figure 2. Rate dependence on [**1**] for the **1**-catalyzed Nazarov cyclization of **2b** in 1:1 D_2O/[D_6]DMSO at 45 °C.

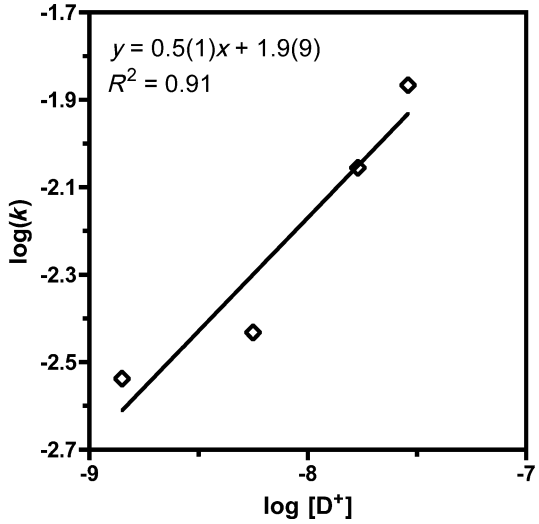

Figure 3. Rate dependence on [D^+] for the **1**-catalyzed Nazarov cyclization of **2b** in 1:1 D_2O/[D_6]DMSO at 45 °C.

reversible binding of substrate, followed by protonation of the bound guest. When the protonation step is made inaccessible by using the less basic substrate **2-CF$_3$**, no reaction occurs.

Further studies of both the **1**-catalyzed and the uncatalyzed reaction were necessary, because these experiments do not provide any information about the reaction mechanism beyond the protonation steps, nor do they suggest which step is rate determining. Earlier studies of the Nazarov cyclization conducted in superacidic media implicate a mechanism in which protonation and water loss is followed by rate-determining electrocyclization of a dienyl cation.[15] Upon quenching, the resulting cyclized allyl cation is deprotonated to give the product cyclopentadiene (Scheme 2). The relative rates of these steps are certainly different under the superacid conditions than they are in aqueous solution (**1** catalyzed or acid catalyzed); for example, **8a** and **9a** were observed by NMR in superacid solution, but not in 1:1 D_2O/[D_6]DMSO at pD 8.0.

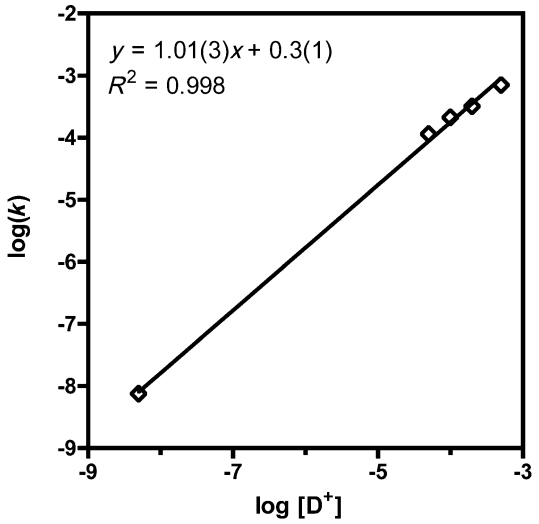

Figure 4. Rate dependence on [D^+] for the uncatalyzed Nazarov cyclization of **2b** in 1:1 D_2O/[D_6]DMSO at 45 °C.

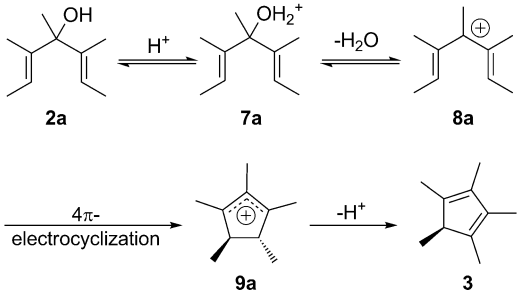

Scheme 2. Proposed mechanism in superacidic solution from Ref. [14].

^{18}O-Incorporation studies

To determine the rate-determining step of the Nazarov cyclization, both the **1**-catalyzed and the acid-catalyzed reaction of **2b** were run to partial conversion in ^{18}O-enriched water. No incorporation of ^{18}O into the recovered starting material would be expected if protonation or water loss is rate-determining, whereas ^{18}O incorporation would be expected if electrocyclization is substantially slower than recombination of carbocation **8a** with water (Scheme 2). Incorporation of ^{18}O into the recovered starting material was observed in both reactions, proving that protonation and water loss are reversible, and in the **1**-catalyzed case, confirming that encapsulation is reversible (Table 2, entries 1–3). No ^{18}O incorporation was observed when the reaction is run at pD 8.0 in the absence of **1**, ruling out any pathway for ^{18}O incorporation that does not involve acid catalysis (Table 2, entry 4).

The rates of ^{18}O incorporation versus the rate of product formation are not equal for the **1**-catalyzed and acid-catalyzed reaction. When the **1**-catalyzed reaction of **2b** was run to 50% conversion, 60% ^{18}O incorporation was observed (Table 2, entry 1). In the acid-catalyzed reaction, 90% ^{18}O incorporation was observed after only 10% conversion, and quantitative incorporation occurred after 50% conversion of **2b** (Table 2, en-

Table 2. The Nazarov cyclization run in $H_2{}^{18}O$/DMSO 1:1.

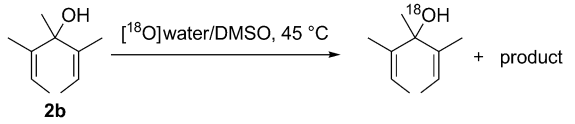

2b

Entry	Catalyst loading	pH	Reaction time [min]	Conversion to product [%]	^{18}O label in **2b** [%]
1[a]	10%	8.0	60	50	60
2	0	3.8	15	10	90
3	0	3.8	60	50	100
4	0	8.0	60	0	0

[a] Reaction run with maleimide co-substrate.

tries 2–3). One explanation for this difference in relative exchange versus cyclization rates is that the recombination of **8b**⊂**1** with water is slower than the analogous reaction of unencapsulated **8b**. It is possible that the effective concentration of water inside the host cavity is lower than in solution, or that **8b** is bound in a conformation that hinders recombination with water. This effect was observed in a previous study, in which the tropylium ion was protected from reacting with water by encapsulation within **1**, dramatically slowing the decomposition rate of the tropylium cation compared to that observed in free solution.[16] A second explanation is that encapsulation lowers the barrier for the electrocyclization of **8b**. Even slightly lowering the 7.1 kcal mol^{-1} barrier calculated for the electrocyclization of **8b** in the catalyzed reaction would account for the observed difference in ^{18}O incorporation. It is not possible to determine which one of these factors is responsible for the ^{18}O incorporation results, or whether both water recombination and electrocyclization are affected by encapsulation. However, it is clear that the barrier for the electrocyclization of **8b**⊂**1** is lowered relative to the recombination of water when compared to unencapsulated **8b**. Additionally, these results indicate that protonation and water loss are rapid compared to electrocyclization in the uncatalyzed reaction, and that electrocyclization is rate determining. In the **1**-catalyzed reaction, the formation of product **4** and labeled reactant **2b**-^{18}O are competitive, so the barrier heights for those two reactions must be similar. That there is no single rate-determining step for the **1**-catalyzed reaction explains the unusual 0.5-order dependence on [D^+] observed in the **1**-catalyzed reaction (Figure 3). These results implicate a mechanism in which reversible substrate binding, protonation, and water loss are followed by irreversible electrocyclization (Figure 5).

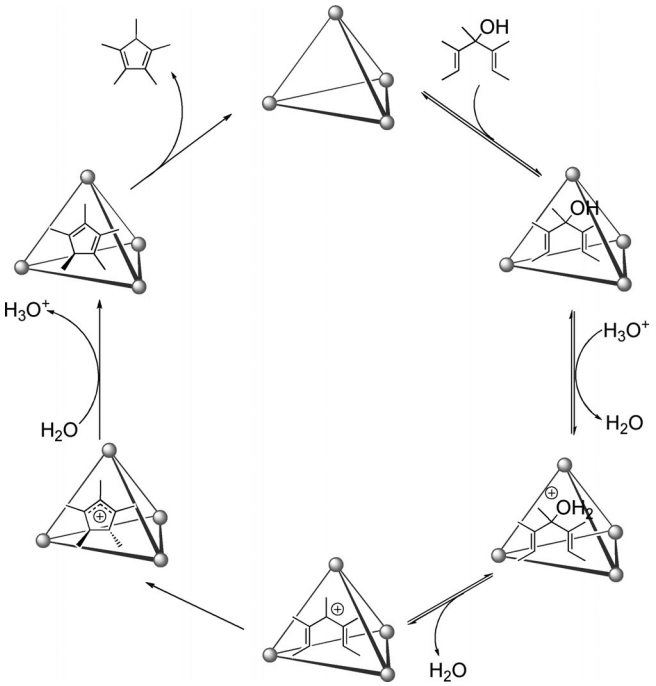

Figure 5. Proposed catalytic cycle for the **1**-catalyzed Nazarov cyclization of 1,4-pentadien-3-ols, with **2a** shown as a representative substrate.

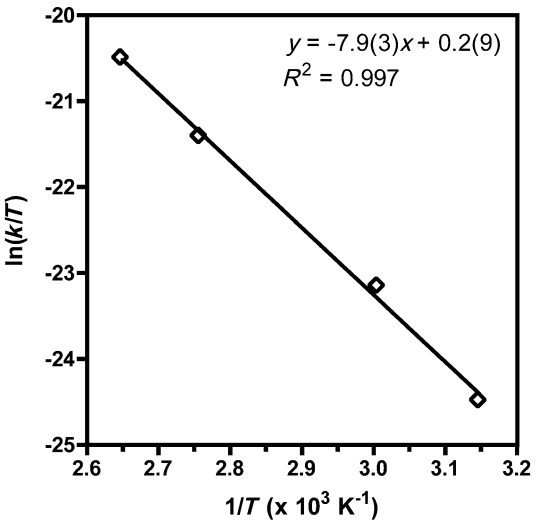

Figure 6. Eyring plot used to determine activation parameters for the uncatalyzed reaction of **2b** (variable-temperature kinetics were conducted between 45 and 105 °C).

Activation parameters

The activation parameters for both the **1**-catalyzed and the uncatalyzed reaction of **2b** were determined to gain additional insight into the origin of the observed rate enhancements. The measured activation parameters for the uncatalyzed reaction of **2b** are $\Delta H^{\ddagger} = 15.6(6)$ kcal mol^{-1} and $\Delta S^{\ddagger} = -47(2)$ e.u. (Figure 6), and the values for the catalyzed reaction of **2b** are $\Delta H^{\ddagger} = 14.8(8)$ kcal mol^{-1} and $\Delta S^{\ddagger} = -20(3)$ e.u. (Figure 7). The $\Delta H^{\ddagger}$ values for both reactions are within the standard error, whereas the entropic barrier is reduced by 28 e.u. in the catalyzed reaction relative to the uncatalyzed reaction. A lowered entropic barrier is consistent with some degree of organization in the transition state of the reaction being provided by encapsulation within **1**; this is the effect that is responsible for catalysis in the **1**-catalyzed aza Cope rearrangement.[5] Protonation of the neutral, encapsulated substrate (**2b**⊂**1**) could also contribute to the lowered entropic barrier; a large, positive change in the entropy of hydration occurs when the host charge is reduced from −12 to −11.[17] However, given that the

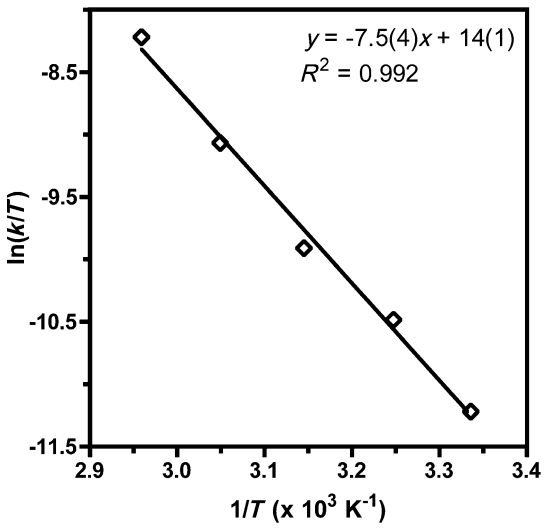

Figure 7. Eyring plot used to determine activation parameters for the **1**-catalyzed reaction of **2b** (variable-temperature kinetics were conducted between 25 and 65 °C).

rate-determining steps for the **1**-catalyzed reaction are different than that of the uncatalyzed reaction, it is possible that the measured activation parameters do not describe identical chemical processes. Thus, the activation parameters for the catalyzed and uncatalyzed reaction may not be directly comparable.

Reaction-energy profile

To gain insight into the dramatic rate acceleration of the Nazarov cyclization that encapsulation in **1** provides, the energetic profiles of the catalyzed and uncatalyzed reaction were estimated and compared. The reactions of **2b** were compared for this purpose, because this substrate was used for the majority of experimental studies. In the uncatalyzed reaction, a pK_a of −5.0 was estimated for protonated **2b** (**7b**), based on comparison to literature values. Accordingly, protonation of **2b** under the experimental conditions, pD 8.0, was estimated to be 18.9 kcal mol^{-1} uphill (for details on estimating the pK_a of **7b**, and for determining the free energy of protonation, see the Supporting Information), but was assumed to have a low additional kinetic barrier (Figure 8). The overall activation energy of 30.4 kcal mol^{-1} for rate-determining electrocyclization was determined from the rate constant of the uncatalyzed reaction. The free energy of intermediate carbocations **8b** and **9a** relative to the transition state of the electrocyclization (−7.1 and −23.1 kcal mol^{-1}, respectively) were predicted by DFT calculations (for details, see the Supporting Information).

The energetic values of binding **2b** in **1** were determined from the self-exchange rate of **2b**⊂**1** ($\Delta G_{exch}^{\ddagger} = 17.0$ kcal mol^{-1}) and the extent to which **2b** is bound by **1** at the beginning of the reaction (Figure 8 represents the beginning of the **1**-catalyzed reaction). Previous studies demonstrated that encapsulation within **1** enhances the basicity of amines by up to 4.5 orders of magnitude, and that this basicity shift is responsible for thousand-fold rate enhancement in the hydrolysis of orthoformates.[7b,8c–e] Accordingly, it was estimated that the acidity of **7b**⊂**1** is four pK_a units higher than that of unencapsulated **7b**, and that protonation of **2b**⊂**1** is 12.7 kcal mol^{-1} uphill. The cation-stabilizing ability of **1** stems from its large negative charge and cation–pi interactions provided by the aromatic rings that comprise the host walls. We assume that the energetic value of water loss from **7b**⊂**1** shown in Figure 8 is 4.4 kcal mol^{-1} uphill, as it is in the uncatalyzed reaction. However, stabilization of the dienyl carbocation **8b** relative to **7b** by encapsulation is certainly possible; earlier studies demonstrated that favoring tropylium in its equilibrium with protonated 2,4,6-cycloheptatrien-1-ol by encapsulation in **1** could play a role in slowing the decomposition of the tropylium ion.[16b] Thus, the energy of **7b**⊂**1** in Figure 8 is a rough estimate. The activation energy of 21.3 kcal mol^{-1} for electrocyclization of **8b**⊂**1** was determined from the rate constant of the **1**-catalyzed reaction. The free energy of **9a**⊂**1** was estimated by assuming moderate binding of **9a** (binding energy of −3.6 kcal mol^{-1} relative to unbound **9a**, corresponding to 10^2 binding). Although this value is speculative, the binding constant is unlikely to be below 10 or above 10^4, a range that includes the majority of cationic guests bound by **1**,[3b,4a,17b,18] and most guests bound by synthetic hosts in general.[19]

In previous studies on the basicity enhancement of **1**-bound guests, the protonation equilibria of bound amines were shifted by a maximum of 4.5 orders of magnitude, and the rate of acid-catalyzed orthoformate hydrolysis was accelerated by a maximum of 3.5 orders of magnitude. Based on this precedent, it is clear that the acceleration of the **1**-catalyzed Nazarov cyclization is not simply due to increasing the basicity of the bound substrate. According to the energetic values estimated for the **1**-catalyzed and uncatalyzed reaction, the reaction barrier for electrocyclization of **8b**⊂**1** is lowered by 3 kcal mol^{-1} relative to **8b** (Figure 8). We considered that either encapsulation within **1** could bind a reactive conformation of **2b** that is disfavored in bulk solution, or that encapsulation could stabilize the transition state itself. Encapsulation in **1** and in other supramolecular assemblies is known to favor folded conformations of acyclic molecules that are otherwise disfavored in bulk solution,[3c,20] and conformational selection is responsible for a nearly thousand-fold rate acceleration in the **1**-catalyzed aza Cope rearrangement of enammonium cations.[5] Examining the rate constants for the uncatalyzed Nazarov cyclization of **2a**, **b**, and **c** indicates that substrate conformation affects the rate of electrocyclization (Table 1); the reaction rate is slowest for **2b**, methyl groups of which are in the *Z* configuration. The *cisoid* conformer of **8b** necessary for rate-determining electrocyclization is sterically disfavored relative to the analogous *cisoid* conformer of **8a**. This effect is relatively small, only lowering the reaction rate of **2b** by a factor of five, relative to that of **2a**, corresponding to an energetic difference of only 1 kcal mol^{-1}. Encapsulation in **1** could further lower the electrocyclization barrier by stabilizing the compact transition state TS2. Based on the small contribution of conformational selection towards the overall rate acceleration, we conclude that transition-state stabilization is the dominant factor in lowering the reaction barrier **8b**⊂**1** relative to **8b**.

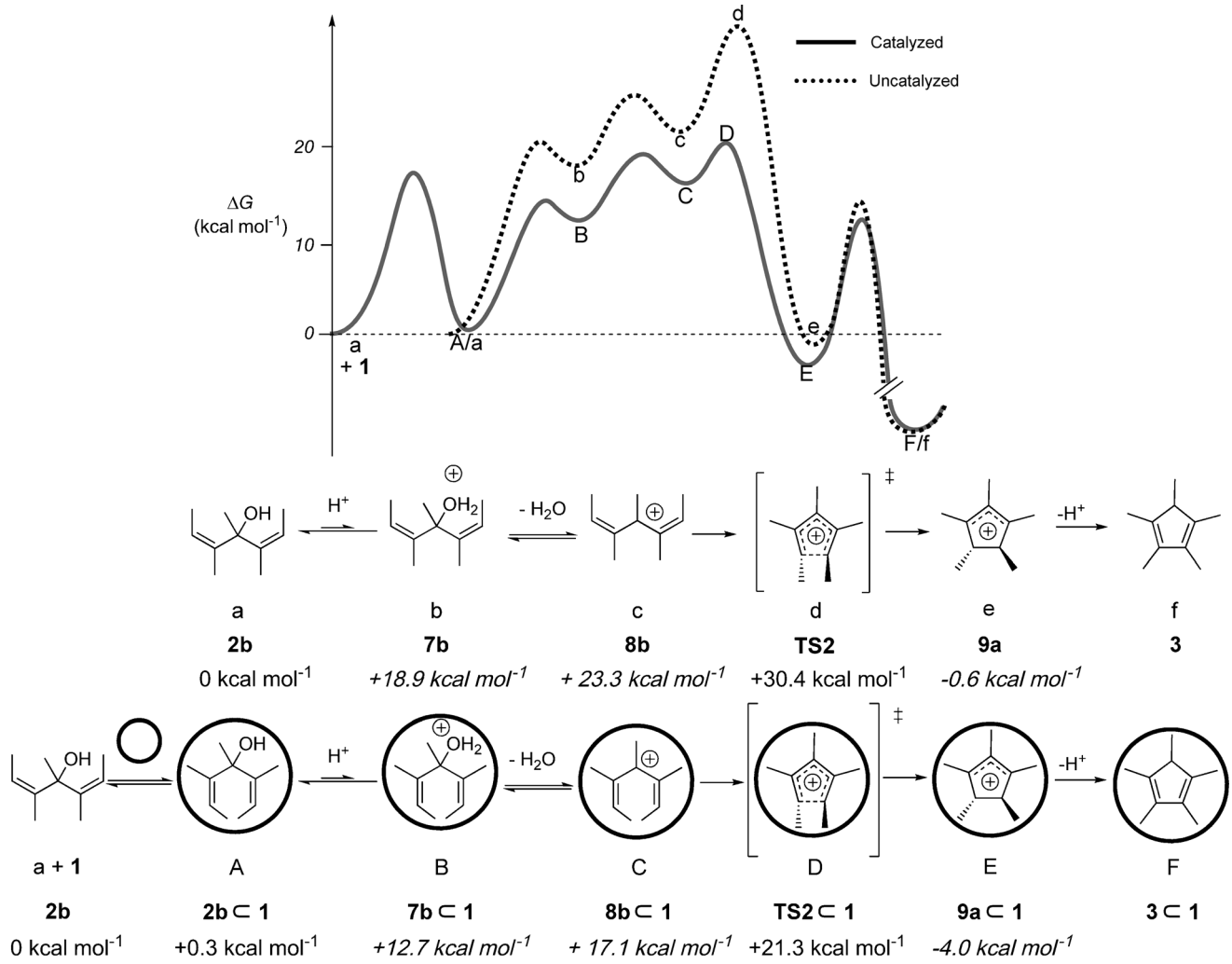

Figure 8. Proposed reaction-coordinate diagram for the **1**-catalyzed and the uncatalyzed Nazarov cyclization of **2b**, showing relative energies at the beginning of the reaction, at 318 K in 1:1 D_2O/[D_6]DMSO with K_3PO_4 (50 mM, pD 8.0), **1** (1.5 mM) and **2b** (25 mM). Energies in italics were estimated (see text).

Conclusion

Mechanistic studies of the **1**-catalyzed Nazarov cyclization of 1,4-pentadien-3-ols were conducted, and comparisons were made to the uncatalyzed reaction to understand the role of encapsulation in this catalysis. Kinetic analysis of the reaction, ^{18}O-exchange experiments, and computational studies imply a mechanism in which encapsulation, protonation, and water loss from substrate are reversible, followed by irreversible electrocyclization. Although electrocyclization is rate determining in the uncatalyzed reaction, the barrier for water loss and for electrocyclization are nearly equal in the **1**-catalyzed reaction. Analysis of the proposed energetics of the catalyzed and uncatalyzed reaction revealed that transition-state stabilization contributes significantly to the catalytic rate acceleration. This, in addition to the enhanced basicity caused by encapsulation in **1**, is responsible for the dramatic million-fold rate enhancement over the uncatalyzed reaction. Comparison of the activation parameters for the catalyzed and uncatalyzed reaction supports the proposed origin of the rate acceleration.

Experimental Section

General

Unless otherwise noted, all reactions and manipulations were performed by using standard Schlenk and high-vacuum techniques at room temperature. All glassware was dried in an oven at 150 °C for at least 12 h or flame dried under vacuum prior to use.

Instrumentation

NMR spectra were obtained on Bruker Avance AVQ 400 (400 MHz), AV 400 (400 MHz), AV 500 (500 MHz), or AV 600 (600 MHz) spectrometers as indicated. Chemical shifts are reported as δ in parts per million (ppm) relative to residual protonated solvent resonances. In the case of D_2O samples, ^{13}C NMR shifts were referenced to an internal standard of CH_3OH.[21] Chemical shifts for ^{19}F NMR data were referenced to an internal standard of trifluoroethanol.[22] NMR data are reported in the following format: (s = singlet, d = doublet, t = triplet, q = quartet, m = multiplet, b = broad; integration; coupling constant). The temperatures of the kinetics experiments carried out in a circulating oil bath were measured by using a calibrated mercury thermometer and varied ±0.1 °C. The temperatures of

the kinetics experiments carried out in an NMR probe were determined from the ^{1}H NMR chemical shifts of ethylene glycol and CH_3OH samples, and varied ± 0.1 °C. Mass spectral data were obtained at the QB3 Mass Spectrometry Facility operated by the College of Chemistry, University of California, Berkeley. Fast atom bombardment (FAB) mass spectra were recorded on a Micromass ZAB2-EQ magnetic sector instrument. Electron impact (EI) and chemical ionization (CI) mass spectra were recorded on a Micromass ProSpec magnetic sector instrument equipped with an EI and a CI source.

Materials

Unless otherwise noted, reagents were obtained from commercial suppliers and used without further purification. Ethyl ether (Et_2O) and tetrahydrofuran (THF) were dried by passing through columns of activated alumina under nitrogen pressure and were sparged with nitrogen before use.[23] $K_{12}Ga_4L_6$ (K_{12}**1**), **2a**, **2b**, and **2c** were prepared according to literature procedures.[3b,9] (*Z*)-2-Bromo-2-butene is occasionally available commercially from Sigma–Aldrich and can be separated from the *E* isomer by preparative gas chromatography.[9]

Synthesis of 4-trifluoromethyl-3,5-dimethylhepta-2-*trans*-5-*trans*-dien-4-one (2-CF_3)

This procedure was adapted for a small scale from a published procedure for the large-scale preparation of **2**.[24] A two-necked round-bottomed flask equipped with a magnetic stir bar and a reflux condenser was charged with lithium wire (155.5 mg, cut into 4 mm lengths, 22.4 mmol) and dry Et_2O (1 mL). (*Z*)-2-Bromo-2-butene was purified and dried immediately before use by passage through a pipette column of basic alumina. The first 0.7 mL of (*Z*)-2-bromo-2-butene (total of 2.0 mL, 11.2 mmol) was added dropwise to the stirred solution by syringe over the course of several minutes. At this point, the reaction initiated, as was indicated by the evolution of heat and bubbling of the reaction mixture. An additional portion of fresh Et_2O (10 mL) was added, and the remainder of the bromide was added slowly to keep the reaction at reflux. After the addition of the bromide was complete, an additional portion of Et_2O (5 mL) was added and stirring was continued for one additional hour. The reaction mixture was then cooled to 0 °C in an ice bath and quenched by the slow addition of ethyl trifluoroacetate (0.7 mL, 5.9 mmol) diluted to 50% with Et_2O. The reaction mixture was poured into saturated aqueous NH_4Cl and extracted five times with Et_2O (20 mL). The combined organic layers were washed with brine and dried over $MgSO_4$, and the solvent was removed by rotary evaporation to obtain the title compound (0.65 g, 3.1 mol) as a yellow liquid in 56% yield and 85% purity. The contaminant is the *E*,*Z* stereoisomer. ^{1}H NMR (400 MHz, $CDCl_3$): $\delta = 5.52$ (q, 2H, $^3J = 7.3$ Hz), 1.87 (s, 6H), 1.60 ppm (d, 6H, $^3J = 7.2$ Hz); ^{13}C{^{1}H} NMR (100.6 MHz, $CDCl_3$): $\delta = 134.1$, 128.7, 126.5 (q, 1C, $^2J_{FC} = 150$ Hz) 78.8 (q, 1C, $^3J_{FC} = 28$ Hz), 22.3 (q, 2C, $^4J_{FC} = 2.7$ Hz), 18.3 ppm; ^{19}F NMR (376.5 MHz, $CDCl_3$): $\delta = -77.58$ ppm (*E*,*Z* stereoisomer at -76.12 ppm); HRMS (EI): elemental analysis calcd (%) for $C_{10}H_{14}F_3O$ $[M-H]^+$: 207.0997; found: 207.0998; elemental analysis calcd (%) for $C_{10}H_{15}F_3O$ $[M]^+$: 208.1075; found 208.1067 (50% intensity with respect to $[M-H]^+$).

Synthesis of K_{12}[2−CF_3⊂1]

The potassium salt of **1** (15.0 mg, 4.0 μmol) was dissolved in D_2O (0.6 mL, buffered to pD 8.0 with 0.1 M KH_2PO_4), and the resulting solution was then mixed thoroughly with **2-CF_3** (2.5 mg, 12.0 μmol). The solution was transferred to an NMR tube, and the spectrum of the host–guest complex was recorded within 20 min. No reaction was observed after the sample was heated at 50 °C for 5 h. Quantitative guest binding was not observed; the binding efficiency is 77%, which represents the relative ^{1}H NMR integrations of the guest to host peaks. The unencapsulated guest is sparingly soluble in D_2O, and only broad resonances were observed. ^{1}H NMR (400 MHz, D_2O): $\delta = 7.94$ (d, 12H, $^3J = 7.7$, Ar-*H*), 7.78 (d, 12H, $^3J = 8.5$ Hz, Ar-*H*), 7.34 (d, 12H, $^3J = 8.2$ Hz, Ar-*H*), 7.01 (t, 12H, $^3J = 8.1$ Hz, Ar-*H*), 6.73 (d, 12H, $^3J = 7.2$ Hz, Ar-*H*), 6.58 (t, 12H, $^3J = 7.8$ Hz, Ar-*H*), −0.90 (d, 3H, $^3J = 7.0$, encaps.), −1.07 (d, 3H, $^3J = 7.0$, encaps.), −1.20 (s, 3H, encaps.), −1.29 ppm (s, 3H, encaps.); ^{19}F NMR (376.5 MHz, D_2O): $\delta = -80.83$ ppm.

General procedure for kinetic runs

In a typical experiment, the substrate (2.0 mg, 13.0 μmol), K_{12}**1** (3.5 mg, 0.9 μmol), maleimide (2.0 mg, 20.6 μmol), and sodium *p*-toluenesulfonate (3.0 mg, 15.4 μmol, added as an integration standard) were dissolved in [D_6]DMSO (0.3 mL) and D_2O (0.3 mL, buffered with 100 mM phosphate buffer, adjusted to the desired pD). The solution was transferred to an NMR tube and inserted into the NMR probe preheated to 45 °C. After allowing the sample temperature to equilibrate for two minutes, ^{1}H NMR spectra were acquired every 20 s, until >95% of the starting material was consumed.

The procedure for sample preparation for uncatalyzed reaction kinetics was analogous to that used for the catalyzed reaction, except that **1** and maleimide were omitted and silylated glassware was used. For experiments conducted at lower pD values (between 3.0 and 4.0), the aqueous portion of solvent was buffered with potassium hydrogen phthalate (100 mM). The sample was sealed under vacuum in a thin-walled NMR tube and heated at 45 °C in a circulating oil bath.

^{18}O-Labeling studies

The procedure for sample preparation was analogous to that used for the kinetic studies: compound **2b** (5.2 mg, 33.7 μmol), K_{12}**1** (3.5 mg, 0.9 μmol), and maleimide (2.4 mg, 24.7 μmol) were dissolved in DMSO (0.3 mL) and [18°]-water (0.3 mL, buffered with 100 mM phosphate adjusted to pH 8.0). The solution was transferred to an NMR tube and heated at 45 °C for one hour in a circulating oil bath. A model reaction by using the same quantity of reagents in deuterated solvents was monitored by ^{1}H NMR, and 50% conversion of starting material was observed after one hour. After heating, the reaction mixture was extracted three times with 0.5 mL portions of ethyl acetate. The combined organic phases were washed three times with brine, dried over $MgSO_4$, and filtered. The resulting solution was analyzed by mass spectrometry (CI) to determine the extent of ^{18}O incorporation. The parent ion of **2** was not observed by other methods of mass spectrometry, such as gas chromatography–mass spectrometry (GC-MS), EI, and FAB. In these experiments, only dehydrated species were observed, and ^{18}O incorporation could not be determined. For the acid-catalyzed and the uncatalyzed reactions, the above-described procedure was followed, except that **1** and maleimide were omitted. [18°]-Water was buffered with potassium hydrogen phthalate (100 mM) for the acid-catalyzed reaction. A model reaction by using the same quantity of reagents in deuterated solvent (aqueous portion buffered to pD 3.4) was monitored by ^{1}H NMR spectroscopy, and 10% conversion of starting material was observed after fifteen minutes, whereas 50% conversion of starting material was observed after one hour.

DFT calculations

All calculations were carried out in the UC Berkeley Molecular Graphics and Computational Facility by using the Gaussian 03 software package with the GaussView graphical user interface.[25] Details are provided in the Supporting Information.

Acknowledgements

The authors would like to thank Dr. Jamin Krinski and Dr. Kathleen Durkin for assistance with DFT computational studies, and acknowledge NSF Grants CHE-0233882 and CHE-0840505, which fund the UC Berkeley Molecular Graphics and Computational Facility. We also thank Dr. Ulla Andersen for obtaining MS data and Prof. Michael Pluth for helpful discussions. We acknowledge financial support from the Director, Office of Science, Office of Basic Energy Sciences, and the Division of Chemical Sciences, Geosciences, and Biosciences of the U.S. Department of Energy at LBNL under Contract No. DE-AC02–05CH11231.

Keywords: carbocations · catalysis · electrocyclization · reaction mechanisms · supramolecular chemistry

[1] H. Dugas, *Bioorganic Chemistry: A Chemical Approach to Enzyme Action*, 3rd ed., Springer, New York, **1999**.

[2] a) J. M. Lehn, C. Sirlin, *J. Chem. Soc. Chem. Commun.* **1978**, 949 – 951; b) G. L. Trainor, R. Breslow, *J. Am. Chem. Soc.* **1981**, *103*, 154 – 158; c) M. W. Hosseini, J. M. Lehn, M. P. Mertes, *Helv. Chim. Acta* **1983**, *66*, 2454 – 2466; d) D. J. Cram, H. E. Katz, *J. Am. Chem. Soc.* **1983**, *105*, 135 – 137; e) M. W. Hosseini, J. M. Lehn, K. C. Jones, K. E. Plute, K. B. Mertes, M. P. Mertes, *J. Am. Chem. Soc.* **1989**, *111*, 6330 – 6335; f) R. Breslow, *Acc. Chem. Res.* **1995**, *28*, 146 – 153; g) A. J. Kirby, *Angew. Chem.* **1996**, *108*, 770 – 790; *Angew. Chem. Int. Ed. Engl.* **1996**, *35*, 706 – 724; h) B. Zhang, R. Breslow, *J. Am. Chem. Soc.* **1997**, *119*, 1676 – 1681; i) R. Breslow, S. Dong, *Chem. Rev.* **1998**, *98*, 1997 – 2011; j) X. Ren, Y. Xue, J. Liu, K. Zhang, J. Zheng, G. Luo, C. Guo, Y. Mu, J. Shen, *Chembiochem* **2002**, *3*, 356 – 363; k) J. Bjerre, C. Rousseau, L. Marinescu, M. Bols, *Appl. Microbiol. Biotechnol.* **2008**, *81*, 1 – 11; l) M. Yoshizawa, J. K. Klosterman, M. Fujita, *Angew. Chem.* **2009**, *121*, 3470 – 3490; *Angew. Chem. Int. Ed.* **2009**, *48*, 3418 – 3438; m) M. J. Wiester, P. A. Ulmann, C. A. Mirkin, *Angew. Chem.* **2010**, *122*, 118 – 142; *Angew. Chem. Int. Ed.* **2010**, *49*, 114 – 137; n) L. Marchetti, M. Levine, *ACS Catal.* **2011**, *1*, 1090 – 1118.

[3] a) T. N. Parac, D. L. Caulder, K. N. Raymond, *J. Am. Chem. Soc.* **1998**, *120*, 8003 – 8004; b) D. Caulder, R. Powers, T. Parac, K. Raymond, *Angew. Chem.* **1998**, *110*, 1940 – 1943; *Angew. Chem. Int. Ed.* **1998**, *37*, 1840 – 1843; c) S. M. Biros, R. G. Bergman, K. N. Raymond, *J. Am. Chem. Soc.* **2007**, *129*, 12094 – 12095.

[4] a) A. V. Davis, D. Fiedler, G. Seeber, A. Zahl, R. van Eldik, K. N. Raymond, *J. Am. Chem. Soc.* **2006**, *128*, 1324 – 1333; b) M. D. Pluth, D. W. Johnson, G. Szigethy, A. V. Davis, S. J. Teat, A. G. Oliver, R. G. Bergman, K. N. Raymond, *Inorg. Chem.* **2009**, *48*, 111 – 120.

[5] a) D. Fiedler, R. G. Bergman, K. N. Raymond, *Angew. Chem.* **2004**, *116*, 6916 – 6919; *Angew. Chem. Int. Ed.* **2004**, *43*, 6748 – 6751; b) D. Fiedler, H. Van Halbeek, R. G. Bergman, K. N. Raymond, *J. Am. Chem. Soc.* **2006**, *128*, 10240 – 10252; c) C. J. Hastings, D. Fiedler, R. G. Bergman, K. N. Raymond, *J. Am. Chem. Soc.* **2008**, *130*, 10977 – 10983.

[6] a) M. Ziegler, J. L. Brumaghim, K. N. Raymond, *Angew. Chem.* **2000**, *112*, 4285 – 42287; *Angew. Chem. Int. Ed.* **2000**, *39*, 4119 – 4121; b) J. L. Brumaghim, M. Michels, K. N. Raymond, *Eur. J. Org. Chem.* **2004**, 4552 – 4559; c) V. M. Dong, D. Fiedler, B. Carl, R. G. Bergman, K. N. Raymond, *J. Am. Chem. Soc.* **2006**, *128*, 14464 – 14465.

[7] a) M. D. Pluth, R. G. Bergman, K. N. Raymond, *Science* **2007**, *316*, 85 – 88; b) M. D. Pluth, R. G. Bergman, K. N. Raymond, *J. Am. Chem. Soc.* **2007**, *129*, 11459 – 11467.

[8] a) J. Ma, D. Dougherty, *Chem. Rev.* **1997**, *97*, 1303 – 1324; b) M. D. Pluth, R. G. Bergman, K. N. Raymond, *Angew. Chem.* **2007**, *119*, 8741 – 8743; *Angew. Chem. Int. Ed.* **2007**, *46*, 8587 – 8589; c) M. D. Pluth, R. G. Bergman, K. N. Raymond, *J. Am. Chem. Soc.* **2008**, *130*, 11423 – 11429; d) M. D. Pluth, R. G. Bergman, K. N. Raymond, *Acc. Chem. Res.* **2009**, *42*, 1650 – 1659; e) M. D. Pluth, R. G. Bergman, K. N. Raymond, *J. Org. Chem.* **2009**, *74*, 58 – 63.

[9] C. J. Hastings, M. D. Pluth, R. G. Bergman, K. N. Raymond, *J. Am. Chem. Soc.* **2010**, *132*, 6938 – 6940.

[10] a) A. Radzicka, R. Wolfenden, *Science* **1995**, *267*, 90 – 93; b) R. Skouta, S. Wei, R. Breslow, *J. Am. Chem. Soc.* **2009**, *131*, 15604 – 15605.

[11] C. J. Hastings, M. P. Backlund, R. B. Bergman, K. N. Raymond, *Angew. Chem.* **2011**, *123*, 10758 – 10761; *Angew. Chem. Int. Ed.* **2011**, *50*, 10570 – 10573.

[12] The self-exchange reaction involves the interchange of encapsulated and non-encapsulated populations of the same guest molecule.

[13] Rate dependence on pD was more convenient to determine at relatively low pD, because the uncatalyzed reaction is extremely slow at basic and near-neutral pD.

[14] a) A. Bondi, *J. Phys. Chem.* **1964**, *68*, 441 – 451; b) M. Charton, *J. Am. Chem. Soc.* **1969**, *91*, 615 – 618; c) K. Uneyama, *Organofluorine Chemistry*, Blackwell, Ames, **2006**.

[15] a) N. C. Deno, C. U. Pittman, *J. Am. Chem. Soc.* **1964**, *86*, 1871 – 1872; b) N. W. K. Chiu, T. S. Sorensen, *Can. J. Chem.* **1973**, *51*, 2776 – 2782.

[16] a) M. Oda, K. Okawa, H. Tsuri, S. Kuroda, *Tetrahedron* **2003**, *59*, 795 – 800; b) J. Brumaghim, M. Michels, D. Pagliero, K. Raymond, *Eur. J. Org. Chem.* **2004**, 5115 – 5118.

[17] C. Sgarlata, J. S. Mugridge, M. D. Pluth, B. E. F. Tiedemann, V. Zito, G. Arena, K. N. Raymond, *J. Am. Chem. Soc.* **2010**, *132*, 1005 – 1009; see also Ref. [3a].

[18] T. Parac, M. Scherer, K. Raymond, *Angew. Chem.* **2000**, *112*, 1288 – 1291; *Angew. Chem. Int. Ed.* **2000**, *39*, 1239 – 1242.

[19] K. N. Houk, A. G.-m. Leach, S. P. Kim, X. Y. Zhang, *Angew. Chem.* **2003**, *115*, 5020 – 5046; *Angew. Chem. Int. Ed.* **2003**, *42*, 4872 – 4897.

[20] a) S. C. Hirst, A. D. Hamilton, *J. Am. Chem. Soc.* **1991**, *113*, 382 – 383; b) A. Scarso, L. Trembleau, J. Rebek, *Angew. Chem.* **2003**, *115*, 5657 – 5660; *Angew. Chem. Int. Ed.* **2003**, *42*, 5499 – 5502; c) D. Ajami, J. Rebek, *J. Am. Chem. Soc.* **2006**, *128*, 15038 – 15039; d) B. Purse, J. Rebek, *Proc. Natl. Acad. Sci. USA* **2006**, *103*, 2530 – 2534; e) J. Rebek Jr., *Chem. Commun.* **2007**, 2777 – 2789; f) D. Ajami, J. Rebek Jr., *Nat. Chem.* **2009**, *1*, 87 – 90.

[21] H. Gottlieb, V. Kotlyar, A. Nudelman, *J. Org. Chem.* **1997**, *62*, 7512 – 7515.

[22] A. A. Ribeiro, M. J. Glen, *J. Magn. Reson. Ser. A* **1994**, *107*, 158 – 166.

[23] P. Alaimo, D. Peters, J. Arnold, R. Bergman, *J. Chem. Educ.* **2001**, *78*, 64 – 64.

[24] R. S. Threlkel, J. E. Bercaw, P. F. Seidler, J. M. Stryker, R. G. Bergman in *Organic Syntheses, Vol. VIII*, Wiley, New York, **1993**, pp. 505 – 508.

[25] Gaussian 03, Revision C.02, M. J. Frisch, G. W. Trucks, H. B. Schlegel, G. E. Scuseria, M. A. Robb, J. R. Cheeseman, J. A. Montgomery, Jr., T. Vreven, K. N. Kudin, J. C. Burant, J. M. Millam, S. S. Iyengar, J. Tomasi, V. Barone, B. Mennucci, M. Cossi, G. Scalmani, N. Rega, G. A. Petersson, H. Nakatsuji, M. Hada, M. Ehara, K. Toyota, R. Fukuda, J. Hasegawa, M. Ishida, T. Nakajima, Y. Honda, O. Kitao, H. Nakai, M. Klene, X. Li, J. E. Knox, H. P. Hratchian, J. B. Cross, V. Bakken, C. Adamo, J. Jaramillo, R. Gomperts, R. E. Stratmann, O. Yazyev, A. J. Austin, R. Cammi, C. Pomelli, J. W. Ochterski, P. Y. Ayala, K. Morokuma, G. A. Voth, P. Salvador, J. J. Dannenberg, V. G. Zakrzewski, S. Dapprich, A. D. Daniels, M. C. Strain, O. Farkas, D. K. Malick, A. D. Rabuck, K. Raghavachari, J. B. Foresman, J. V. Ortiz, Q. Cui, A. G. Baboul, S. Clifford, J. Cioslowski, B. B. Stefanov, G. Liu, A. Liashenko, P. Piskorz, I. Komaromi, R. L. Martin, D. J. Fox, T. Keith, M. A. Al-Laham, C. Y. Peng, A. Nanayakkara, M. Challacombe, P. M. W. Gill, B. Johnson, W. Chen, M. W. Wong, C. Gonzalez, J. A. Pople, Gaussian, Inc., Wallingford CT, **2004**.

Received: October 3, 2013
Published online on February 25, 2014

